Spectral measurement of absorption by spectroscopic frequency-domain optical coherence tomography

R. Leitgeb

Institute of Medical Physics, University of Vienna, Waehringer Strasse 13, A-1090 Vienna, Austria

M. Wojtkowski and A. Kowalczyk

Institute of Physics, Nicholas Copernicus University, ulica Grudziadzka 5/7, Pl-87-100 Torun, Poland

C. K. Hitzenberger, M. Sticker, and A. F. Fercher

Institute of Medical Physics, University of Vienna, Waehringer Strasse 13, A-1090 Vienna, Austria

Received January 19, 2000

A new method of measurement that essentially combines Fourier-domain optical coherence tomography with spectroscopy is introduced. By use of a windowed Fourier transform it is possible to obtain, in addition to the object structure, spectroscopic information such as the absorption properties of materials. The feasibility of this new method for performing depth-resolved spectroscopy is demonstrated with a glass filter plate. The results are compared with theoretically calculated spectra by use of the well-known spectral characteristics of the light source and the filter plate. © 2000 Optical Society of America

OCIS codes: 110.4500, 110.6960, 120.3180, 300.1030, 300.0300.

Optical coherence tomography (OCT) provides noninvasive morphological cross-sectional information on biological tissues and materials.[1] Spectroscopic OCT is attractive because it combines spectral tissue-extinction data with the optical path length of the photons propagating through the tissue, a prerequisite for quantitative spectroscopic data.[2] In a first study of spectroscopic OCT the complete complex envelope of the depth-scan signal at a wavelength of 1.3 μm over a bandwidth of approximately 50 nm was used.[3] A related technique, absorption-sensitive OCT imaging, is based on a dual-wavelength OCT system; this technique has already been used for measuring the local concentration of water in an intralipid phantom.[4] In a more recent study of spectroscopic OCT an ultrabroadband femtosecond Ti:sapphire laser was used to achieve spectroscopic imaging over a wavelength range from 650 to 1000 nm.[5]

The spectroscopic OCT techniques mentioned above use standard OCT, in which depth (z) resolution is obtained from a low-coherence-interferometry depth scan and transverse resolution is obtained by lateral scanning of the object with a narrow probe beam. In this Letter we present spectroscopic frequency-domain OCT, a new spectroscopic OCT technique, and describe its application to measurement of depth-resolved spectral absorption. In this technique, too, transverse resolution is obtained by lateral scanning of the object by a narrow probe beam. However, in frequency-domain OCT, depth resolution is obtained from backscattering spectral interferometry.[6] Here the backscattered light wave is detected at a range of wave numbers K by use of an interferometer together with a spectrometer. Hence there is direct access to spectroscopic data.

Backscattering spectral interferometry is based on a solution of the inverse scattering problem presented by Wolf.[7] He showed that some of the Fourier components of a weakly scattering object can be obtained from measurements of the scattered field. Furthermore, it has been shown that, in the far field, the electric field $E_O(K)$ of the light that is scattered back in the z direction is a traveling wave, $E_O(K) \propto A_O(K)\exp(-ikz - i\omega t)$, where, besides a proportionality factor, the amplitude of this wave equals the Fourier transform of the scattering potential $F_O(z)$ of the object,[8] $A_O(K) \propto \mathrm{FT}[F_O(z)]$. The quantity $F_O = -K^2[m^2(z) - 1]$ represents the scattering potential of the object, $m(z)$ is the complex refractive index, and $K = 2k = 4\pi/\lambda$ is the scattered wave number. The object potential $F_O(z)$ is obtained by an inverse Fourier transform of the K-number-resolved amplitude $A_O(K)$ of the backscattered object wave. In spectroscopic frequency-domain OCT the K spectrum $A_O(K)$ of the backscattered light is measured in the same way as in frequency-domain OCT, by use of a spectrometer at the interferometer exit (see Fig. 1). But rather than Fourier

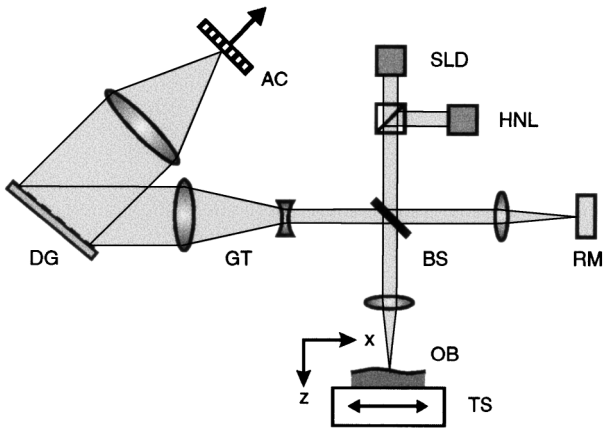

Fig. 1. Optical scheme for spectroscopic frequency-domain OCT. See text for other definitions.

0146-9592/00/110820-03$15.00/0

transformation of the complete spectrum in one step, a frequency window $g(\Delta K; K_n)$ of width ΔK centered at a mean scattering wave number K_n is shifted along the spectrum step by step, and the spectral data within the windows are Fourier transformed:

$$\mathrm{FT}^{-1}[A_O(-K)g(K_n; \Delta K)] = F_O(z; K_n) * [\hat{g} \exp(iK_n z)], \tag{1}$$

where $\hat{g}$ represents the Fourier-transformed window function. Hence we obtain the scattering potential with a point spread function determined by the spectral width ΔK and a phase factor determined by the mean wave number. One has to choose the window function g appropriately to reduce spectral leakage effects.

The result of this procedure is a series of object potentials $F_O(z; K_n)$ that are associated with each spectral window centered at K_n. Thus one obtains a spectral plot of the scattering potential as a function of z as well as of K_n. The resolutions in z and K space are related by the uncertainty relation $\Delta K \Delta z \geq 1/4\pi$ (for Gaussian windows, this relation becomes an equality). Hence, if one wants to increase the spectroscopic resolution by using small windows (small ΔK), one effectively loses spatial depth resolution (large Δz).

A straightforward implementation of this technique requires K-dependent measurement of both the amplitudes and the phases of the backscattered waves. However, we only have access to the wave-number-dependent intensity spectrum $I_O(K)$, which is proportional to the square of the Fourier transform $\hat{F}_O(K)$ of the scattering potential of the object:

$$I_O(K) = |E_O(K)|^2 = C|\hat{F}_O(K)|^2, \tag{2}$$

where C is a proportionality factor. Taking the inverse Fourier transform of $I_O(K)$ yields the autocorrelation function (ACF) of the scattering potential:

$$\mathrm{FT}^{-1}[I_O(K)] = C\langle F_O{}^*(z), F_O(z + Z)\rangle = C \times \mathrm{ACF}_F(Z). \tag{3}$$

Autocorrelation is not reversible. If, however, a reference mirror at z_R (with amplitude reflectivity R) is provided, the autocorrelation contains one term that yields a reconstruction of the complex object structure, centered at $z = z_R$, i.e., $RF_O(z + z_R)$.[8]

Figure 1 depicts the optical scheme of the spectroscopic frequency-domain OCT device. A superluminescent diode [SLD (EG&G C86142)] with $\lambda = 830$ nm, $\delta\lambda$ (FWHM) = 25 nm, and 1-mW output power is used as a light source in a Michelson interferometer. A He–Ne laser (HNL) is used for adjustment purposes. A beam splitter (BS) directs one beam to the reference mirror (RM) and the other to the object (OB). The object is mounted on a translation stage (TS) for transverse scanning. The transverse resolution is given by the beam waist in the focal plane of the object arm, which amounts to 200 μm. The two beams that are reflected from the reference arm and the object arm are expanded by a Galilean telescope (GT) and directed to the diffraction grating [DG (Zeiss; 1800/mm)]. The diffracted beams are spectrally displayed by a lens (120-mm achromat) on the CCD sensor (AC) of a digital camera (Hamamatsu C4249-95; 1024 × 1024 pixels). The camera detects the wavelength-dependent intensity spectrum of the interferogram formed by the superposition of the backscattered object wave with the reference wave. The dispersion of the diffraction grating and the fact that the recorded light spectrum diffracted from the diffraction grating is a function of wavelength λ rather than of wave number K are sources of nonlinearities that have to be numerically compensated for.

For the spectroscopic measurements a glass plate (BK7) of 1-mm geometric thickness was used first to demonstrate that reflections from both the front and the back surfaces show essentially the same spectral characteristic, namely, the Gaussian characteristic of the superluminescent diode. Since the glass plate is only 1 mm thick, dispersion effects are of minor importance in this case and should not cause any difference in the spectra reflected by the front and back surfaces. To obtain a spectral OCT image of the glass plate we scanned the object transversely along a 2-mm line in 50-μm steps. The windowed Fourier transform (WFT) of the numerically compensated spectrum at one transverse point yields a two-dimensional intensity plot, where the object function (as a function of depth coordinate z) is found to be parallel to the ordinate and the spectral intensity (as a function of λ) is found to be parallel to the abscissa (Fig. 2). Hence it is possible to extract the intensity spectrum at one point of a particular reflecting surface of the object, where the spectral resolution is determined mainly by the chosen WFT window length. This procedure has to be repeated for each transverse point, yielding a set of spectra that one can combine to yield the OCT image shown in Fig. 3(a). For the WFT a Blackman window of 400 points proved to be best for the present setup; i.e., it provided the best signal-to-noise ratio and vanishing signal distortion.

As a preliminary test of the feasibility of this method we apply the same procedure to investigate

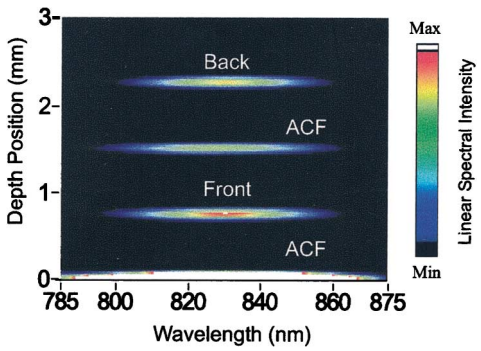

Fig. 2. WFT plot at one transverse point of a 1-mm BK7 glass plate. The lines labeled ACF represent the autocorrelation functions of the glass plate. Back and front denote the surface reflections.

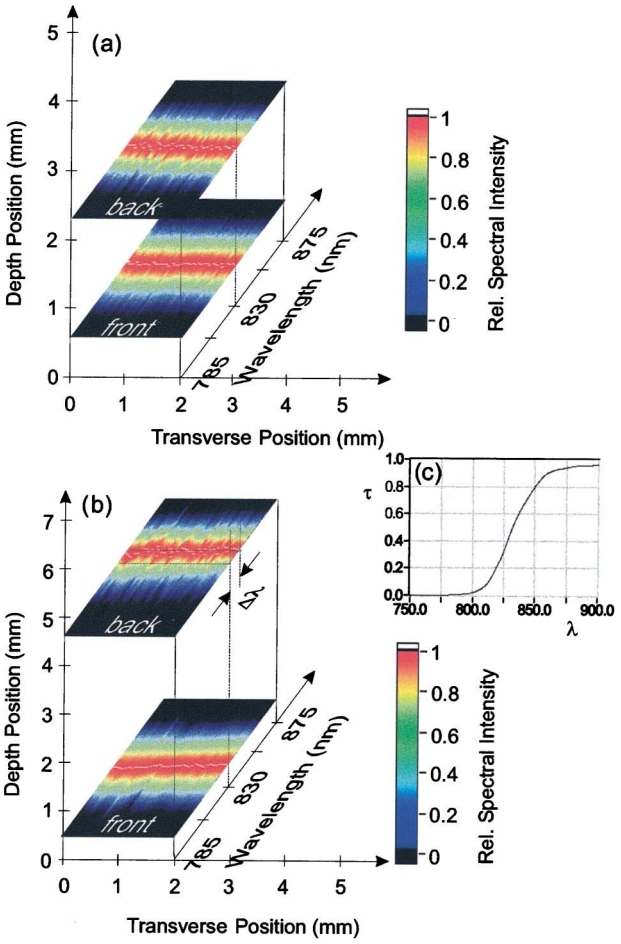

Fig. 3. Spectral OCT images of (a) a BK7 glass plate and (b) a RG830 glass filter plate. The spectra are normalized to their respective peak values. (c) Transmission curve for the RG830 filter plate (transmission τ versus wavelength λ).

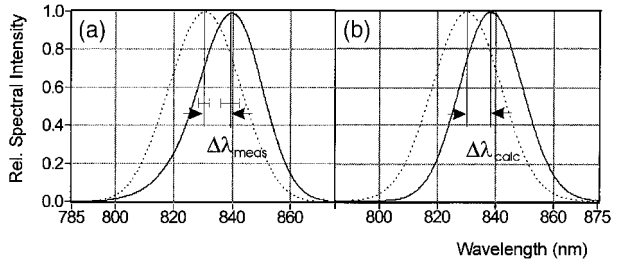

Fig. 4. (a) Measured spectra at (dotted curve) the front and (solid curve) rear surfaces of the RG830 filter. The error bars indicate the standard deviations of the peak positions along the wavelength axis. (b) Calculated spectra. $\Delta\lambda_{meas}$ and $\Delta\lambda_{calc}$ are the respective redshifts in the spectra of the light reflected at the back surface.

a simple absorbing object. An IR glass filter plate (Linos RG830) with transmittance $\tau = 0.5$ at $\lambda = 830$ nm and a geometric thickness of 3 mm serves as the object [Fig. 3(c)]. As in the case of the glass plate, the filter plate was scanned transversely along a 2-mm line in 50-μm steps. Again, from the WFT at each transverse scanning point it is possible to extract the spectra of light reflected from the front and back surfaces of the filter plate. The spectral OCT image of the filter plate is shown in Fig. 3(b), in which the spectra are normalized to their respective peak values. Since the filter attenuates shorter wavelengths more strongly than longer ones, one would expect a shift of the spectral weight toward longer wavelengths. This effect is nicely demonstrated by the measurement [$\Delta\lambda$ in Fig. 3(b) and $\Delta\lambda_{meas}$ in Fig. 4(a)] and can be compared with the calculated shift $\Delta\lambda_{calc} = 8.4$ nm in Fig. 4(b). For the calculation we used the known spectral characteristics of the superluminescent diode and the RG830 filter plate. We obtained the results shown in Fig. 4(a) by averaging the spectra along the transverse 2-mm line at the front and rear surfaces separately. The redshift $\Delta\lambda_{meas}$ amounted to 9.2 ± 1.9 nm, where the error was calculated from the standard deviations of the respective peak positions along the wavelength axis.

As mentioned above, there is a trade-off between spectral resolution ΔK and longitudinal resolution Δz. From the point of view of spectroscopy it would clearly be interesting to make ΔK as small as possible. However, besides loss of longitudinal resolution with increased spectral resolution, the smaller the window, the more prominent the noise effects become, which eventually results in heavy distortion of the spectra. Nevertheless, this new method can be seen to provide a simple and fast way of investigating the absorption properties of material layers.

This project was financed by the Austrian Fonds zur Förderung der wissenschaftlichen Forschung (grant P 10316 MED) and the Trans-European Mobility Programme for University Studies. R. Leitgeb's e-mail address is rainer.leitgeb@univie.ac.at.

References

1. A. F. Fercher, J. Biomed. Opt. **1,** 157 (1996).
2. D. A. Benaron, W. E. Benitz, R. L. Ariagno, and D. K. Stevenson, Clin. Pediatr. **31,** 258 (1992).
3. M. Kulkarni and J. A. Izatt, in *Conference on Lasers and Electro-Optics*, Vol. 9 of 1996 OSA Technical Digest Series (Optical Society of America, Washington, D.C., 1996), pp. 59–60.
4. J. M. Schmitt, S. H. Xiang, and K. M. Yung, J. Opt. Soc. Am. A **15,** 2286 (1998).
5. U. Morgner, F. X. Kartner, S. H. Cho, Y. Chen, H. A. Haus, J. G. Fujimoto, E. P. Ippen, V. Scheuer, G. Angelow, and T. Tschudi, Opt. Lett. **24,** 411 (1999).
6. A. F. Fercher, C. K. Hitzenberger, G. Kamp, and S. Y. El-Zaiat, Opt. Commun. **117,** 43 (1995).
7. E. Wolf, Opt. Commun. **1,** 153 (1969).
8. A. F. Fercher and C. K. Hitzenberger, in *International Trends in Optics and Photonics (ICO IV)*, T. Asakura, ed., Vol. 4 of Springer Series in Optical Sciences (Springer-Verlag, Berlin, 1999), pp. 359–389.
9. A. F. Fercher, R. Leitgeb, C. K. Hitzenberger, H. Sattmann, and M. Wojtkowski, Proc. SPIE **3564,** 173 (1999).